Available online at www.sciencedirect.com
ScienceDirect
Geochimica et Cosmochimica Acta 71 (2007) 5044–5053
Geochimica et Cosmochimica Acta
www.elsevier.com/locate/gca

Aqueous uptake of uranium onto pyrite surfaces; reactivity of fresh versus weathered material

T.B. Scott *, O. Riba Tort, G.C. Allen

University of Bristol, Interface Analysis Centre, 121 St. Michael's Hill, Bristol BS2 8BS, UK

Received 25 May 2007; accepted in revised form 6 August 2007; available online 14 September 2007

Abstract

In order to better understand the interaction between aqueous uranium and pyrite (FeS_2) the uptake of uranium onto the surfaces of both weathered and freshly generated pyrite surfaces was examined using batch sorption experiments. Analysis was performed using X-ray photoelectron spectroscopy (XPS). The results clearly indicate that freshly polished pyrite surfaces are efficient scavengers of uranium from solution, while weathered surfaces exhibit only limited uptake. Results also indicate partial reduction of uranium at the pyrite surfaces, with a heterogeneous distribution of U(IV) and U(VI) species.

1. INTRODUCTION

Pyrite (FeS_2) is the most common and arguably the most interesting of all the sulphide minerals. It is found in a wide range of geological settings such as soils, metamorphic zones, ore deposits and anoxic sedimentary environments and as such has attracted considerable research effort aimed at fully determining its surface properties and reactivity within the environment. Pyrite is common as both a primary and secondary mineral component in sedimentary rocks and soils (Berner, 1984), and often coexists with other desirable minerals such as gold, copper and lead.

The behaviour of pyrite in the near surface geosphere is of great environmental concern. When pyrite is exposed to aerated aqueous solutions at atmospheric conditions, it oxidatively decomposes; releasing dissolved ferrous iron, H^+ ions, sulphite, thiosulphate and sulphate into solution (Chen and Morris, 1972; Lowson, 1982; Goldhaber, 1983; Moses et al., 1987). This cocktail of oxidation products is commonly referred to as acid mine drainage and poses a large environmental problem in mining areas and estuarine sediments where toxic heavy metals such as As, Cd, Pb and Zn can be liberated into ground and surface waters. (Lowson, 1982; Goldhaber, 1983; Moses et al., 1987; Morse et al., 1987; Pain et al., 1998).

With regard to the occurrence of uranium in the natural environment, pyrite has been reported in association with uranium ore deposits in both metamorphic and sedimentary settings (Simpson and Bowles, 1977; Cunningham et al., 1998; England et al., 2001). The most common sedimentary uranium deposits occur in organic-rich and frequently pyrite-rich black shales, exemplified by the Randstad Shales of Sweden (Swanson, 1956) and the Chattanooga and the New Albany Shales of the USA (Nash et al., 1981). Typically, these deposits contain low levels of uranium (2–4 ppm), although a direct association of uranium with both organic matter and pyrite was identified, citing absorption as the vehicle for uranium concentration (Swanson, 1956).

More recently, work concerned with the environmental remediation and retardation of aqueous uranium at contaminated sites has focused on the use of iron-bearing minerals such as magnetite, hematite and goethite (Hsi and Langmuir, 1985; Lenhart and Honeyman, 1999; Dodge et al., 2002; Missana et al., 2003; Scott et al., 2003). Work reported by Wersin et al. (1994) has also identified pyrite as a medium for the uptake and possible reduction of U(VI) compounds. The study proposed that partial reduction to uranium U(IV) may be correlated with the oxidation

* Corresponding author.
E-mail address: T.B.Scott@bristol.ac.uk (T.B. Scott).

0016-7037/$ - see front matter © 2007 Elsevier Ltd. All rights reserved.
doi:10.1016/j.gca.2007.08.017

state of the pyrite surface, based on an apparent correlation of U sorption sites with pyrite oxidation zones.

The classical bulk reaction of aqueous uranium with pyrite is thought to be as follows:

$$2FeS_2 + UO^{2+}_{2[aq]} + 2H_2O + 7O_2 \Rightarrow 2Fe^{3+} + 4SO^{2-}_4 + UO_{2[s]} + 4H^+ \quad (1)$$

This reaction implies a reductive precipitation mechanism, where aqueous U(VI) is reduced and removed from solution as a U(IV) solid in UO_2 on the pyrite surface. However, pyrite surface reactivity is rather more complicated with the potential for uranium remediation via a number of different mechanisms, predominating under different pH and redox conditions.

1. *Reductive precipitation* of uranium coupled to the oxidation of Fe(II) to Fe(III). Reduction of U(VI) to U(IV) would result in the precipitation of non-stoichiometric UO_2.
2. *Reductive precipitation* of uranium coupled to the oxidation of sulphide to polysulphide and/or sulphur. Reduction of U(VI) to U(IV) would again result in the precipitation of non-stoichiometric UO_2.
3. *Co-precipitation* and *Structural incorporation* of U(VI) during the formation of iron oxides, elemental sulphur and other sulphate species at the pyrite surface. A reaction similar to that observed for goethite, haematite and rust phases.

Lalou et al. (1996) have shown that in a natural system, uranium uptake by sulphides occurs during and/or very soon after their formation and that the resulting uranium content is a function of local environmental conditions.

The chemical nature of pyrite surfaces pre-, syn- and post-oxidation has previously been reported by numerous XPS studies, of which all demonstrate that oxidation of fresh pyrite surfaces produces iron oxides, elemental sulphur and sulphate species (Buckley and Woods, 1987; Hyland and Bancroft, 1989; Mycroft et al., 1990; Karthe et al., 1993; Nesbitt and Muir, 1994; Knipe et al., 1995). The fundamental mechanisms involved in the oxidative dissolution and decomposition of pyrite, directly relate to those governing uranium sorption.

The purpose of this current study was to more fully elucidate the interaction between aqueous uranium and the surfaces of weathered and freshly polished pyrite using sorption studies involving both X-ray photoelectron spectroscopy (XPS). The experimental data was intended to expand upon the findings of Wersin et al. (1994).

1.1. Pyrite structure and surface chemistry

In order to better understand the interaction between aqueous uranium and both weathered and freshly polished (or fresh) pyrite surfaces, it is first necessary to understand the structure and chemistry of pyrite. Two structural environments must be considered, the 'bulk' crystal structure and the structure local to the crystal surface.

Bulk pyrite can be considered to have a modified face-centred cubic rocksalt (NaCl) structure with Fe in the Na site positions and covalently bonded S_2 pairs in the Cl positions.

Bond strength is known to be proportional to the electron density at the bond critical point (bcp) and is inversely related to bond length (Feynman, 1939; Knop et al., 1988). In the pyrite structure, the S–S bond (2.08 Å) is observed to be shorter and more strongly covalent than the Fe–S bond (2.26 Å), suggesting that it has greater strength. Analysis of the critical point properties of the pyrite bonds (Rosso, 1998) also suggests this, indicating that the valence electron density at the S–S bcp is 29% higher than that for the Fe–S bond. Given that the S–S bond is stronger than the Fe–S bond, crystal cleavage should not result in the pervasive breakage of S–S bonds, suggesting that nearer equal proportions of 'dangling' Fe and S bonds may be generated at the cleaved surface, and readily react with any suitable species in order to regain charge stability and bonding symmetry.

1.2. Surface oxidation

As previously discussed, the removal of uranium from solution onto pyrite may be linked to oxidative corrosion of the mineral surface. Should the surface already have experienced corrosion (i.e. it is weathered) it may be passive to uranium sorption reactions. On this basis is it important to gain an understanding of pyrite oxidation and resultant reaction products. Pyrite undergoes a complex cycle of reactions during aqueous oxidation. The initial step in pyrite oxidation is considered to involve the oxidation of the sulfur to sulfate, releasing Fe^{2+} into solution where it can be oxidized by molecular oxygen to Fe^{3+} (Eqs. 2 and 3). At near neutral pH the ferric ion will almost all be precipitated as iron oxide or hydroxide:

$$2FeS_2 + 2H_2O + 7O_2 \rightarrow 2Fe^{2+} + 4SO^{2-}_4 + 4H^+_{(aq)} \quad (2)$$

$$4Fe^{2+} + 4H^+_{(aq)} + O_2 \rightarrow 4Fe^{3+} + 2H_2O \quad (3)$$

Ferric iron may act as an electron acceptor for further pyrite oxidation (4), or hydrolysis may occur (5), both processes releasing further protons:

$$FeS_2 + 14Fe^{3+} + 8H_2O \rightarrow 15Fe^{2+} + 2SO^{2-}_4 + 16H^+_{(aq)} \quad (4)$$

$$Fe^{3+} + 3H_2O \rightarrow Fe(OH)_3 + 3H^+_{(aq)} \quad (5)$$

The overall sequence of reactions is acid-producing (Banks et al., 1997), and can be summarized in the following form:

$$4FeS_2 + 14H_2O + 15O_2 \rightarrow 4Fe(OH)_3 + 8SO^{2-}_4 + 16H^+_{(aq)} \quad (6)$$

The oxidation reactions listed above (Eqs. (2)–(6)) are now well-established due to many years of research summarised in reviews by Hiskey and Schlitt (1981); Lowson (1982) and Nordstrom (1982). Additionally, isotopic tracer studies (Taylor and Wheeler, 1984; Reedy et al., 1991) have shown that water participates more as a reactant and less as a spectator species during aqueous pyrite decomposition, with rapid hydroxylation of active surface sites.

X-ray photoelectron spectroscopy has been the primary tool used for elucidation of the sub reactions and oxidation products appearing at a pyrite surface. Numerous studies have reported that surface oxidation of pyrite occurs heterogeneously or incompletely, with many intermediate oxidation products, including elemental sulphur, thiosulphate, and polysulphides being retained on the pyrite surface (Chen and Morris, 1972; Lowson, 1982; Goldhaber, 1983; Moses et al., 1987). Based on the change in aqueous oxidation products observed with time, it is generally accepted that oxidation of pyrite results in the formation of ferric (hydroxyl)sulphates and discrete Fe-oxyhydroxide patches or a Fe-oxyhydroxide layer (Nicholson et al., 1988; Nicholson et al., 1990) (Fig. 1).

What is unclear, however, is the order in which oxidation products develop at the pyrite surface. The general observation is that oxidation products occur on the pyrite surface in the order: iron oxides and/or hydroxides, iron sulphate and an iron deficient sulphide layer (Fig. 2a) (Buckley and Woods, 1987; Hyland and Bancroft, 1989; Mycroft et al., 1990; Karthe et al., 1993; Nesbitt and Muir, 1994; Knipe et al., 1995). This order would indicate that iron is the more reactive of the two elemental species, during oxidation, with S oxidation products such as sulphate developing later. This is also in agreement with the different bond strengths reported for Fe–S and S–S bonds. Indeed, the rate and extent of pyrite oxidation is thought to be limited by the oxidation of Fe^{2+} to Fe^{3+} because molecular oxygen reacts very slowly with disulphide iron (Singer and Stumm, 1970; Luther, 1987).

Other more recent studies have proposed that S_2^{2-} at the pyrite surface is considerably more reactive than previously thought. Observations suggest that S_2^{2-} on fractured pyrite surfaces is rapidly destroyed (80% within 1 min of air exposure), forming sulphate as the initial oxidation product, with iron oxyhydroxide developing later as a subsidiary phase (Schaufuss et al., 1998a) (Fig. 2b). Nesbitt et al. (2000) supplemented these findings by proposing that the rupture of S–S bonds during fracture produces S^{1-} moieties, which are subsequently reduced to S^{2-} with coupled oxidation of Fe^{2+} to Fe^{3+}.

Reaction conditions such as temperature and pH provide the greatest control on surface oxidation, and dictate which oxide products develop. A recent study by Todd et al. (2003) used synchrotron-based X-ray absorption spectroscopy to examine the nature of surface oxidation phases on pyrite reacted in both air and aqueous conditions. In air-saturated solutions below pH 4, ferric (hydroxyl) sulphate was observed as the primary oxidation product, while at higher pH iron (III) oxyhydroxide was identified on the surface in addition to ferric (hydroxyl)sulphate. Under the most alkaline conditions goethite was reported as the dominant oxidation product.

With regard to uranium uptake onto pyrite surfaces, it is thought that the accumulated thickness and chemistry of any surface oxide phases will directly affect the rate and amount of uranium sorbed, acting as a passive, protective coating. Recent work (Scott, 2005) has highlighted a significant difference in the amounts of uranium removed from solution by weathered and freshly crushed granular pyrite. Flow-through column experiments run for a two week period recorded uranium uptake values of 0.897 and 7.44 mg/m^2, respectively for the two materials. Solution analysis also indicated that the residual filtrate was enriched in sulphur (9.8 and 6.8 ppm, respectively) while iron concentrations showed no significant increase (0.2 and 0.6 ppm, respectively).

The current work provides a surface science study of uranium uptake onto weathered and freshly polished pyrite surfaces using X-ray photoelectron spectroscopy. The objective of the study was to determine the reason for the difference in pyrite reactivity and identify the mechanisms responsible for uranium uptake.

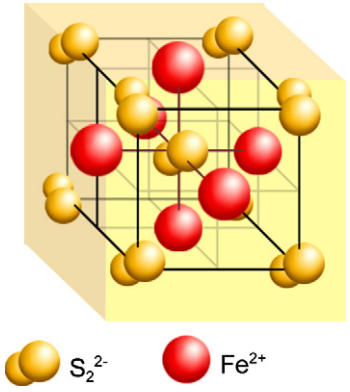

Fig. 1. FeS_2 cubic crystal structure.

2. EXPERIMENTAL

2.1. Analytical techniques

Analysis of pyrite surfaces exposed to uranyl solutions was performed using X-ray photoelectron spectroscopy.

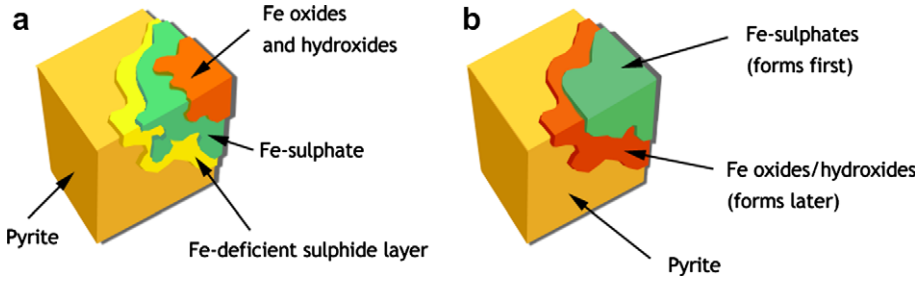

Fig. 2. Diagrams representing the two models proposed for the development of oxidation products on pyrite.

Table 1
Binding energies (eV) reported for the U $4f_{7/2}$ peak in U(IV) and U(VI) oxides

	Allen et al. (1974a)	Chadwick (1973)	Wersin et al. (1994)	
U(IV) as UO_{2+x}	380.6	380.7	380.8	eV
U(VI) as UO_3	381.9	381.9	382.4	eV

Photoelectron spectra were recorded using a Thermo VG Scientific X-ray photoelectron spectrometer (XPS) using Al-Kα (1486.6 eV) radiation at 400 W (15 kV). High-resolution scans were acquired with a 30 eV pass energy, and 200 ms dwell times. All binding energies were referenced to the adventitious hydrocarbon C 1s line at 284.8 eV.

The relative surface concentrations of U(IV) and U(VI) on the pyrite surface were determined using curve fitting of the U 4f photoelectron lines (Chadwick, 1973; Allen et al., 1974a). The peaks resulting from the U 4f core level can be quantitatively resolved into U(VI) and U(IV) components based on the binding energies of uranium reported in the literature (Table 1). Since the binding energy of UO_2 is lower than that of UO_3, a shift or broadening of the U 4f peaks to lower energies can be interpreted as the reduction of U(VI) to a lower oxidation state.

Quantitative measurements of atomic percentage were obtained for U, S, Fe and O using wide scan photoelectron spectra generated by Al-Kα radiation. Relative errors were calculated at less than $\pm$3.5% for U, $\pm$5.2% for S, $\pm$6.8% for Fe and $\pm$3.2% for O, using the method of Harrison and Hazell (1992). Quantitative analysis was performed by comparison of peak areas and atomic concentrations were calculated using selected photoelectron peaks and their associated sensitivity factors (Wagner, 1988).

It should be noted that the XPS technique is only slightly less surface specific than secondary ion mass spectrometry (SIMS). Using either Mg or Al X-ray sources the analysis depth of photoelectron spectroscopy is a maximum of 10 nm. This means that quantitative measurements are only representative of the uppermost 10 nm of the surface of the sample analysed.

Solution pH was monitored at regular periods throughout the experiments to provide an indication of chemical changes within the system.

2.2. Experimental method

Sectioning natural pyrite crystals along the cubic 100 crystal planes using a water-cooled silicon carbide cutting disc created a series of 18 pyrite coupons for analysis each approximately 8 mm square. A group of 9 'fresh' samples were then prepared by wet-grinding under ambient laboratory conditions using progressively finer Beuhler SiC grit papers, achieving a 4000 grade finish (~1–2 μm). A single polished sample was immediately analysed as an unreacted standard using XPS while the other 8 polished samples were immediately exposed to 10 ml of 10 ppm uranyl acetate solution at 20 °C, in individual polythene vials. Pairs of samples were left to react for 12, 24, 48 and 168 h, respectively. The pH of the 10 ppm U stock solution was recorded at pH 4.80.

The second group of 9 samples were placed in an environmental chamber for a 168 h period in order to 'weather' the sample surfaces prior to uranium reaction. The chamber temperature was maintained at 20 °C, with 60% humidity and 400 ppm CO_2 for the duration of the 'weathering' process. Subsequently, 8 of these samples were exposed to 10 ml of 10 ppm uranyl acetate solution in individual polythene vials. Pairs of samples were reacted for 12, 24, 48 and 168 h, respectively. The final 'weathered' sample was analysed as an unreacted standard using XPS. Sample solutions were gently agitated for the duration of the experiment using an automated rocker set at 20 rpm. The surfaces of the unreacted standards were also examined using a scanning electron microscope (SEM).

After suitable exposure each coupon was removed from solution, briefly washed in deionised water to remove any unbound (absorbed or physisorbed) uranyl species and dried, taking care to avoid contamination or disruption of the surface. Samples were then mounted and analysed under high vacuum (better than 5×10^{-8} mbar) using XPS. The pH of the residual U solutions was subsequently measured and recorded.

3. RESULTS AND DISCUSSION

3.1. Starting materials

SEM examination of freshly polished and weathered samples (Fig. 3) highlighted differences between the sample surfaces. At very high magnification freshly polished pyrite surfaces revealed a finely abraded surface with numerous elongate pits, steps and angular depressions aligned with crystal orientation. By comparison, the surfaces of weathered samples were considerably less angular, with pitted and stepped areas of the samples being partially rounded or fragmented. Amorphous growth patches of secondary phases draped the sample surfaces with isolated occurrences of hexagonal, tabular crystals up to 4 μm in diameter growing from the sample surfaces.

Comparison of the XPS data recorded from freshly polished and weathered samples indicated that sample weathering resulted in the development of iron (III) oxide and sulphate phases at the pyrite surfaces (Fig. 4). Photoelectron spectra recorded from different regions of the same weathered sample showed marked differences in the relative abundances of iron oxide and sulphate, indicating spatial heterogeneity. The primary S 2p peaks recorded from weathered samples were shifted by ~0.5 eV to higher binding energy, relative to freshly polished samples, indicating the presence of polysulphide species at the sample surfaces (Hyland and Bancroft, 1989; Mycroft et al., 1990; Nesbitt and Muir, 1994).

Both SEM and XPS analysis indicated significant differences in the topographic and chemical character of the pyrite samples. On this basis alone, it was expected that the

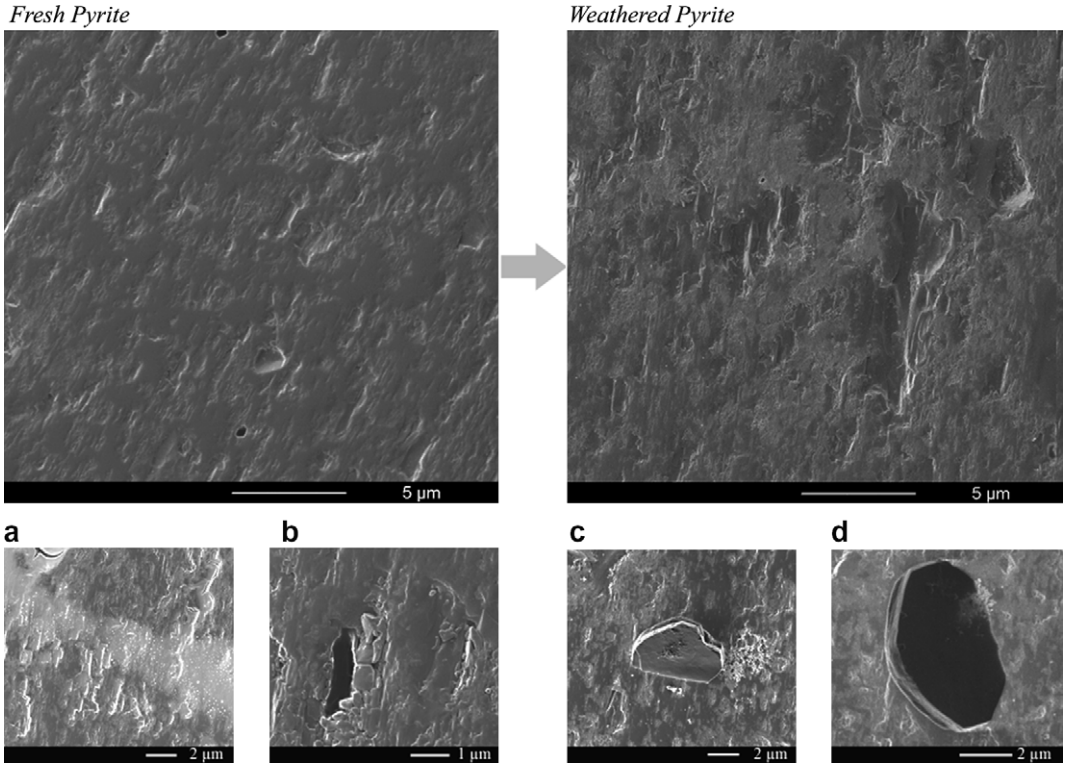

Fig. 3. Secondary ion images of the surfaces of freshly polished and weathered pyrite surfaces. Samples were'weathered' in an environmental chamber at 20 °C, 60% humidity and 400 ppm CO_2 for a 168 h period.

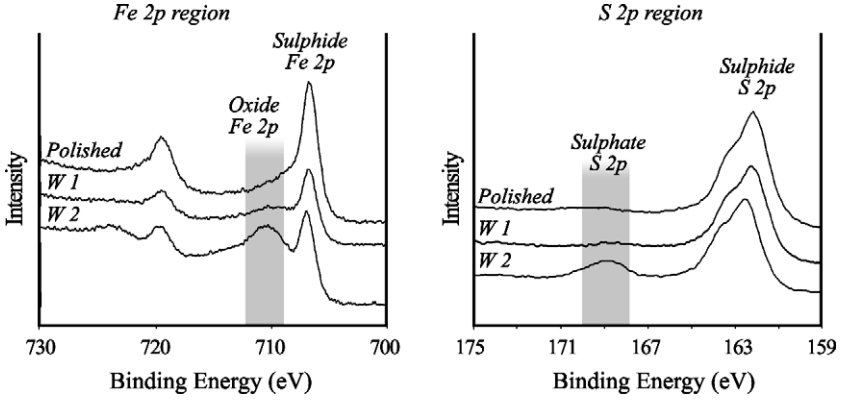

Fig. 4. Fe 2p and S 2p photoelectron regions recorded from the surfaces of freshly polished and weathered pyrite samples. Two different spectra are displayed from the weathered pyrite sample (W1 and W2) reflecting the heterogeneity of surface chemistry. Both iron (III) oxide and sulphate species were recorded at the surface of the weathered material.

different types of pyrite surface would react differently with aqueous uranium.

3.2. Quantitative XPS analysis

The amounts of U recorded on sets of polished and weathered pyrite samples after exposure to U solution were significantly different (Fig. 5).

With up to 168 h exposure to 10 ppm U solution, weathered pyrite surfaces displayed only a limited amount of U sorption, with >90% of sorption observed to occur within the first 12 h of exposure. The quantitative data provided no significant evidence for continued accumulation of surface U to 168 h exposure. A mean uranium abundance of 0.27 at% was recorded from the weathered samples.

Freshly polished pyrite surfaces were observed to exhibit a significant amount of U sorption within the first 12 h of solution exposure, reaching abundances of 1.5 at%. Subsequently, from 12 to 168 h reaction time the amount of uranium detected on the sample surfaces was observed to increase at an hourly accumulation rate of 0.007 at%. After 168 h reaction the polished samples recorded surface U

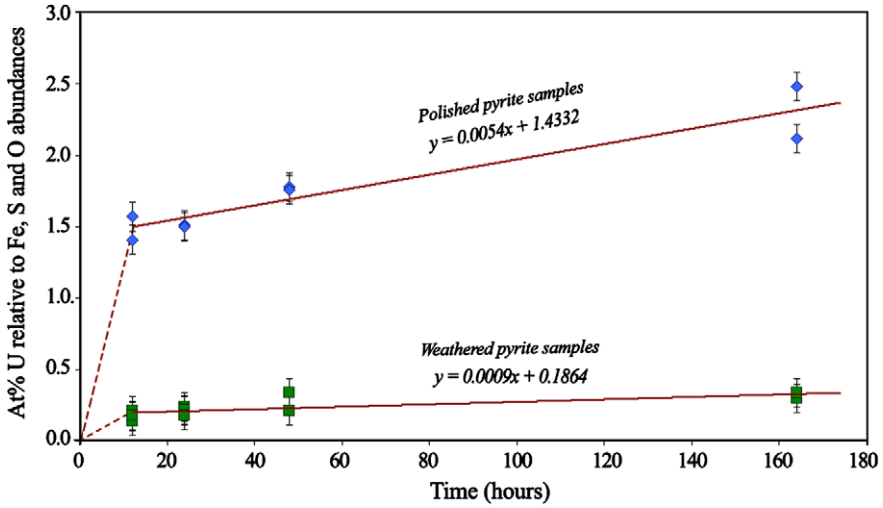

Fig. 5. A comparison of U abundance (at%) detected at fresh and weathered pyrite surfaces after reaction with 10 ppm U solution at initial pH 4.8, for periods up to 168 h. Relative Atomic percentages were calculated for U, Fe, S and O detected at the pyrite surfaces using XPS data.

abundances of 2.6 at%, which was approximately ten times the maximum amount observed for weathered pyrite surfaces.

A comparison of the relative concentration (at%) of Fe, S and O determined from XPS wide scan spectra indicated that the surface chemistry of weathered and polished pyrite samples was markedly different prior to reaction (Fig. 6).

Quantification of the measurements obtained from non-reacted weathered samples indicated relatively high O concentrations (~50 at%) and low Fe concentrations (~10 at%), reflecting the presence of sulphate SO_4^{2-} species at the sample surfaces. Within the first 24 h of reaction, weathered samples displayed a relative increase in Fe abundance to ~18 at%, coupled with a decrease in O abundance to less than 30 at%. From 48 to 168 h, O concentration showed a gradual increase of ~3 at%, while Fe concentrations showed little variation. S concentration recorded an increase of 15 at% over the first 48 h of reaction, with a subsequent decrease of 2–3 at% by 168 h. The observed trend is interpreted as indicating dissolution of surface sulphate species within the first 24 to 48 h of reaction, followed by a more gradual oxidation of Fe^{2+} and S^{-1} exposed at the pyrite surface.

Quantification of the measurements obtained from polished samples also indicated a rapid change in surface chemistry within the first 24 h of solution exposure. This was marked by a 20 at% decrease in S abundance with a coupled 12 at% increase in O concentration and 5 at% increase in Fe. Subsequently, O concentration were observed to increase reaching 39 at% by 168 h while Fe and S concentrations showed a further decrease to 13 at% and 45 at%, respectively. The changes in relative concentrations (at%) of Fe, S and O recorded from the surfaces of polished pyrite samples clearly indicate the progressive development of oxide phases on the surface.

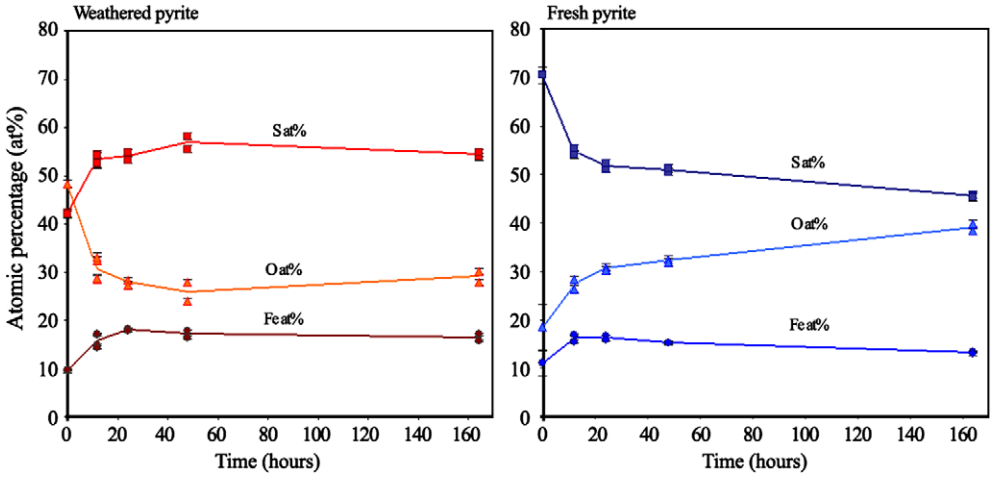

Fig. 6. A comparison of Fe, S and O abundances (at%) detected on polished and weathered pyrite surfaces at different reaction times with 10 ppm U solution at initial pH 4.8, for periods up to 168 h.

3.3. Photoelectron peak analysis (XPS)

The S 2p photoelectron lines recorded from the two sets of reacted pyrite samples showed very little difference after 12 h reaction (Fig. 8). The primary S 2p line was observed at a binding energy of 162.4 eV ±0.15 for all 12 h samples, with similar spectral intensities recorded for each set of samples (Fig. 7).

In comparison to XPS data recorded from unreacted samples, the S 2p lines recorded for the polished pyrite after 12 h reaction displayed a small 0.3 eV shift to higher binding energy and broadening of the recorded line, indicating an increasing proportion of surface polysulphide and oxidation of S_2^{2-} to S_{2+x}^{2-}.

Sulphate species previously identified on weathered samples prior to reaction with U solution were not identified at the sample surfaces after any of the reaction periods. It is suggested that the pH of the U solution (pH 4.8) was sufficient to facilitate the dissolution of surface sulphate species within the first 12–24 h of exposure as indicated by XPS. This was also indicated by ICP-AES data obtained from previous studies of uranium sorption onto pyrite (Scott, 2005).

The S 2p lines recorded from samples reacted for 168 h were observed at the same binding energy (162.4 eV) as those recorded after 12 h reaction. The relative intensity of lines recorded from polished samples had decreased by ~30%, with no appreciable decrease observed for the weathered samples.

The Fe 2p lines recorded from the two sets of pyrite samples after 12 h were dominated by intense Fe 2p3/2 and 2p1/2 peaks at 707.0 and 719.7 eV, respectively (Fig. 8), typical of Fe^{2+} in the FeS_2 lattice (Hyland and Bancroft, 1989; Mycroft et al., 1990; Nesbitt and Muir, 1994; Wersin et al., 1994). The presence of small amounts of surface Fe-oxide was indicated by a low, broad peak in the tail region to the high binding energy side of the primary Fe 2p peaks. This secondary set of peaks at 710.8 and 724.1 eV (±0.2), were at binding energy values typical of Fe(III) in iron oxide or oxyhydroxide phases. By 168 h of reaction the weathered pyrite samples recorded only Fe(III) at the sample surfaces indicating increased surface oxidation (Eq. (6)). Polished pyrite samples also recorded increased amounts of surface iron oxide.

Analysis of the O 1s regions of the photoelectron spectra recorded from the samples provided valuable confirmation of the types of oxide phases developing on the different pyrite samples. Spectra recorded from all the samples reacted for 12 h showed O 1s peaks that were slightly asymmetrical to the high binding energy side and centred at 531.9 eV

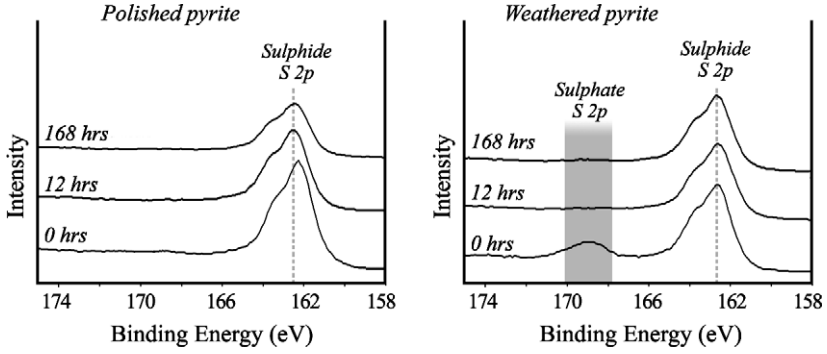

Fig. 7. Photoelectron spectra of S 2p lines recorded from polished and weathered pyrite surfaces reacted with 10 ppm U solution for 12, 48 and 168 h.

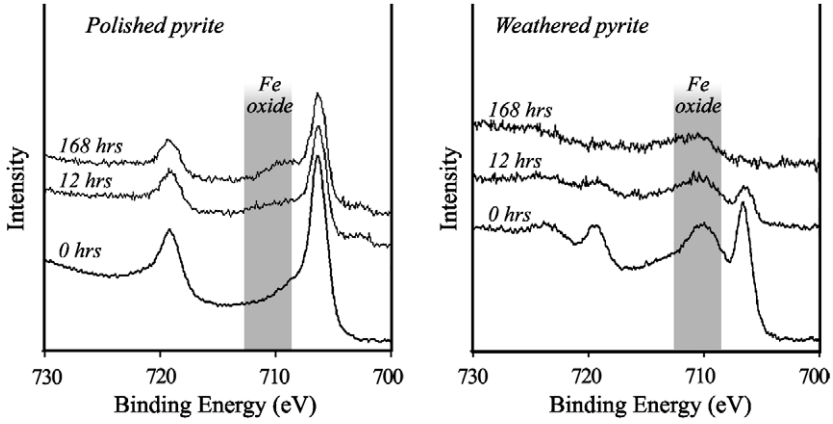

Fig. 8. Photoelectron spectra of Fe 2p lines recorded from polished and weathered pyrite surfaces reacted with 10 ppm U solution for 12 and 168 h. The spectra are displayed with those recorded from untreated surfaces.

(±0.2), with very similar spectral intensities (not shown in this article).

Samples reacted for 168 h showed a marked difference between polished and weathered samples. Polished pyrite samples recorded a slight shift of the O 1s line to lower binding energy at 531.5 eV (±0.2) with an accompanying increase in spectral intensity. Conversely, the spectra recorded from weathered samples displayed no significant change from those recorded after 12 h reaction time.

The U 4f photoelectron spectra recorded from U-reacted polished surfaces showed relatively intense U 4f lines. At 12 h reaction time, the U 4f lines were centred at binding energy values of 381.9 and 392.7 eV (±0.2) closely matching values reported for U(VI) (Chadwick, 1973; Allen et al., 1974a) and were asymmetric to the low binding energy side (Fig. 9). Samples reacted for 48 h showed increased proportions of U(IV) and by 168 h U 4f lines closely matched those previously reported for U(IV) in non-stoichiometric UO_2 (Chadwick, 1973; Allen et al., 1974a). The gradual shift in binding energy of the U 4f lines provides strong evidence to indicate surface sorption of U(VI) and subsequent reduction of the reaction period to U(IV).

Polished samples reacted for 168 h also showed the development of well defined satellite peaks 6.0 eV (±0.2) to the high binding energy side of the primary U 4f lines. The relative locations of the satellite peaks in the U 4f spectrum were in very close agreement with those observed for UO_2 by Verbist et al. (1976) and Allen et al. (1981) and provided further evidence for the presence of hyperstoichiometric UO_{2+x} on the pyrite surfaces.

Curve fitting of the recorded U 4f lines for the polished samples indicated an overall increase in the proportion of U(IV) relative to U(VI) with increasing reaction time. However, a variance of up to 20% in the U(VI):U(IV) ratios was recorded from different areas of the same samples, indicating that the spatial distribution of U(VI) and U(IV) species was variable on the pyrite surfaces. Even after 168 h reaction time, fitting results still indicated some presence of U(VI) indicating that surface reduction of uranium was partial.

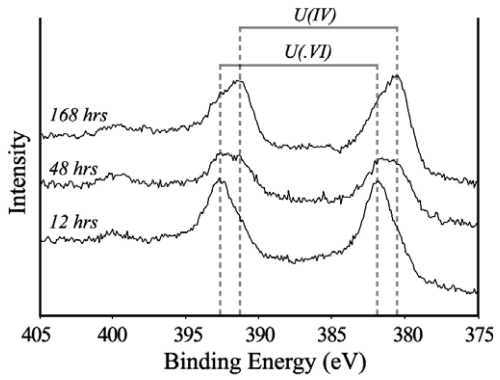

Fig. 9. Photoelectron spectra of U 4f lines recorded from polished pyrite surfaces reacted with 10 ppm U solution for 12, 48 and 168 h. An increasing proportion of U(IV) was observed with increasing reaction time.

The photoelectron spectra recorded from weathered pyrite surfaces displayed very weak U 4f lines, centred at binding energies of 380.8 and 391.8 eV, respectively. Determination of U(VI):U(IV) ratios was not possible due to the low intensity of the U 4f lines, although the peak centres recorded indicated the presence of partially reduced uranium oxide.

The XPS data clearly indicates a significant difference in surface reactivity of the polished and weathered pyrite samples towards the uptake of aqueous uranium. It is suggested that the reaction of weathered pyrite samples with aqueous uranium was limited by the presence of a passive surface layer, consisting of a heterogeneous mix of Fe(III) oxide, polysulphide and sulphate (Chen and Morris, 1972; Lowson, 1982; Goldhaber, 1983; Moses et al., 1987). This 'weathered' layer showed very little reaction with aqueous U, attributed to the fact that the constituent phases themselves were in a partially or fully oxidised chemical state. Disappearance of S 2p peaks attributed to sulphate on the reacted weathered samples indicated early dissolution of surface sulphate, which was consistent with geochemical expectations given the pH of the reactant solutions. Loss of surface sulphate was not observed to significantly improve U uptake onto the residual material.

The XPS data also indicates that gradual oxidation of the weathered surfaces continued throughout the experiment, evidenced by an increasing amount of surface Fe(III) and decreasing amount of disulphide iron recorded in the Fe 2p photoelectron region. It is suggested that continued pyrite oxidation proceeded via reaction of O_2 (Eq. (6)) rather than aqueous U(VI). This is evidenced by the lack of uranium detected at the weathered sample surfaces at the end of the reaction period which suggests that uranium was not readily included in the oxidation reactions.

The location of U 4f lines recorded from the weathered samples after reaction indicates that U(VI) was the predominant surface species most likely associated with hydrated iron oxide phases via sorption or incorporation. Some partial uranium reduction to form UO_{2+x} was indicated by the data.

In contrast to the weathered pyrite samples the XPS data provides a clear indication of more significant uranium uptake and reduction at the surface of the freshly polished pyrite samples. The data indicates the rapid surface oxidation of sulphur from S_2^{2-} to S_{2+x}^{2-} and more gradual oxidation of Fe(II) to Fe(III) forming iron oxides and oxyhydroxides. Either of these reactions may be attributable (and coupled) to the reductive precipitation of UO_2 observed.

3.4. Solution analysis

The pH values recorded for each reacted solution showed very little variation, staying within 0.05 of the initial value (pH 4.80). This result was not unsurprising given the small surface area of the sample relative to solution volume.

4. CONCLUSIONS AND IMPLICATIONS

The development of a weathered layer on the pyrite surfaces prior to reaction was found to significantly limit the

amount of uranium sorption observed. Given that pyrite surfaces in natural systems are more likely to have surfaces which are weathered rather than freshly exposed; the enhanced uptake of uranium by fresh pyrite surfaces observed in this study is not likely to be significant in natural systems. On this basis it is expected that pyrite present in the near-surface geosphere proximal to radionuclide storage sites will exhibit only very limited uranium uptake under near-neutral groundwater conditions. In large this will be due to the presence of passive surface coatings on the pyrite grains although the abundance of dissolved carbonate in contaminated groundwaters would be expected to remain a significant limiting effect on uranium sorption.

It has been clearly demonstrated that polished or 'fresh' pyrite surfaces are considerably more efficient scavengers of uranium from solution than 'weathered' counterparts. The XPS data clearly shows the presence of non-stoichiometric UO_2 at the mineral surface, indicating that surface reduction of U(VI) to U(IV) had occurred. The data also indicates a minor presence of U(VI) at the mineral surfaces indicating that reduction is not uniform. Variations in the relative proportions of U(IV) and U(VI) across the sample surface indicates that the relative distribution of uranium is heterogeneous. These findings are in good agreement of those of Wersin et al. (1994) who also proposed partial reduction of uranium at the pyrite surface and correlated uranium distribution with zones of pyrite oxidation.

From the data presented it may be argued that deliberate activation of pyrite surfaces, either by fracturing or polishing could provide a means of effective uranium remediation. Future work will examine the sorption of uranium onto 'fresh' pyrite across a range of pH in order to examine the optimal conditions for sorption and surface reduction. However, it is suggested that pyrite would not be suited for use as a reactant material for 'in situ' remediation of uranium contaminated sites or aquifers. The primary reason for this recommendation is the inherent and well-documented problems with environmental oxidation of pyrite, causing acidification of groundwaters and resultant remobilisation of toxic heavy metals through dissolution.

REFERENCES

Allen G. C., Tucker P. M. and Tyler J. W. (1981) Satellite structure in the U 4f X-ray photoelectron spectrum of uranium dioxide. *J. Chem. Soc. Chem. Commun.* **397**, 691–692.

Allen G. C., Crofts J. A., Curtis M. T., Tucker P. M., Chadwick D. and Hampson P. J. (1974a) X-ray photoelectron spectroscopy of some uranium oxide phases. *J. Chem. Soc. Dalton* **12**, 1296–1301.

Banks D., Younger P. L., Arnese R. T., Iversen E. R. and Banks S. B. (1997) Mine-water chemistry: the good, the bad and the ugly. *Environ. Geol.* **32**(3), 157–174.

Berner R. A. (1984) Sedimentary pyrite formation: an update. *Geochim. Cosmochim. Acta* **48**, 605–615.

Buckley A. N. and Woods R. (1987) The surface oxidation of pyrite. *Appl. Surf. Sci.* **27**, 437–452.

Chen K. Y. and Morris J. C. (1972) Kinetics of oxidation of aqueous sulphide by oxygen. *Environ. Sci. Technol.* **6**, 529–537.

Chadwick D. (1973) Uranium 4f binding energies studied by X-ray photoelectron spectroscopy. *Chem. Phys. Lett.* **21**, 291–294.

England G. L., Rasmussen B., Krapez B. and Groves D. I. (2001) The origin of uraninite, bitumen nodules and carbon seams in the Witwatersrand gold–uranium–pyrite ore deposits, based on a Permo-Triassic analogue. *Econ. Geol.* **96**, 1907–1920.

Cunningham C. G., Rasmussen J. D., Steven T. A., Rye R. O., Rowley P. D., Romberger S. B. and Selverstone J. (1998) Hydrothermal uranium deposits containing molybdenum and fluorite in the Marysvale volcanic field, west-central Utah. *Miner. Deposita* **33**, 477–494.

Dodge C. J., Francis A. J., Gillow J. B., Halada G. P., Eng C. and Clayton C. R. (2002) Association of uranium with iron oxides typically formed on corroding steel surfaces. *Environ. Sci. Technol.* **36**, 3504–3511.

Feynman R. P. (1939) Forces in molecules. *Phys. Rev.* **56**, 340–343.

Goldhaber M. B. (1983) Experimental study of metastable sulphur oxyanion formation during pyrite oxidation at pH 6–9 and 30 °C. *Am. J. Sci.* **283**, 193–217.

Harrison K. and Hazell L. B. (1992) The determination of uncertainties in quantitative XPS/AES and its impact on data acquisition strategy. *Surf. Interf. Anal.* **18**, 368–376.

Hiskey J. B. and Schlitt W. J. (1981) Aqueous oxidation of pyrite. In *Proceedings of the 2nd SME-SPE International Solution Mining Symposium*, Denver, CO, pp. 55–74.

Hsi C. D. and Langmuir D. (1985) Adsorption of uranyl onto ferric oxyhydroxides. Application of the surface complexation site-binding model. *Geochim. Cosmochim. Acta* **49**, 1931–1941.

Hyland M. M. and Bancroft G. M. (1989) An XPS study of gold deposition at low temperatures on sulphide minerals: reducing agents. *Geochim. Cosmochim. Acta* **53**, 367–372.

Karthe S., Szargan R. and Suoninen E. (1993) Oxidation of pyrite surfaces: a photoelectron spectroscopic study. *Appl. Surf. Sci.* **72**, 157–170.

Knipe S. W., Mycroft J. R., Pratt A. R., Nesbitt H. W. and Bancroft G. M. (1995) X-ray photoelectron spectroscopic study of water adsorption of iron sulphide minerals. *Geochim. Cosmochim. Acta* **59**, 1079–1090.

Knop O., Boyd R. and Choi S. C. (1988) Sulfur–sulfur bond lengths, or can a bond length be estimated from a single parameter? *J. Am. Chem. Soc.* **110**, 7299.

Lalou C., Reyss J. L., Brichet E., Krasnov S., Stepanova T., Cherkashev G. and Markov V. (1996) Initial chronology of a recently discovered hydrothermal field at 14°45′N, Mid-Atlantic Ridge. *Earth Planet. Sci. Lett.* **144**, 483–490.

Lenhart J. J. and Honeyman B. D. (1999) Uranium (VI) sorption to hematite in the presence of humic acid. *Geochim. Cosmochim. Acta* **63**, 2891–2901.

Lowson R. T. (1982) Aqueous oxidation of pyrite by molecular oxygen. *Chem. Rev.* **82**, 461–497.

Luther, III, G. W. (1987) Pyrite oxidation and reduction: molecular orbital theory considerations. *Geochim. Cosmochim. Acta* **51**, 3193–3199.

Missana T., Maffiotte C. and García-Gutiérrez M. (2003) Surface reactions kinetics between nanocrystalline magnetite and uranyl. *J. Colloid Interf. Sci.* **261**, 154–160.

Morse J. W., Millero F. J., Cornwell J. C. and Rickard D. (1987) The chemistry of the hydrogen sulfide and iron sulfide systems in natural waters. *Earth Sci. Rev.* **24**, 1–24.

Moses C. O., Nordstrom D. K., Herman J. S. and Mills A. L. (1987) Aqueous pyrite oxidation by dissolved oxygen and by ferric iron. *Geochim. Cosmochim. Acta* **51**, 1561–1571.

Mycroft J. R., Bancroft G. M., McIntyre N. S., Lorimer J. W. and Hill I. R. (1990) Detection of sulphur and polysulphides on electrochemically oxidized pyrite surfaces by X-ray photoelectron spectroscopy and Raman spectroscopy. *J. Electroanal. Chem.* **292**, 139–152.

Nash J. T., Granger H. C. and Adams S. S. (1981) Geology and concepts of genesis of important types of uranium deposits. *Econ. Geol.*, 63–116, 75th ann. vol..

Nesbitt H. W. and Muir I. J. (1994) X-ray photoelectron spectroscopic study of a pristine pyrite surface reacted with water vapor and air. *Geochim. Cosmochim. Acta* **58**, 4667–4679.

Nesbitt H. W., Scaini M., Höchst H., Bancroft G. M., Schaufuss A. G. and Szargan R. (2000) Synchrotron XPS evidence for Fe^{2+}–S and Fe^{3+}–S surface species on pyrite fracture-surfaces, and their 3D electronic states. *Am. Mineral.* **85**, 850–857.

Nordstrom K. D. (1982) Aqueous pyrite and the consequent formation of secondary minerals. In *Acid Sulfate Weathering: Pedogeochemistry and Relationship to Manipulation of Soil Materials* (eds. J. A. Kittrick, D. S. Fanning and L. R. Hossner). Soil Science Society of America Press, Madison, Wisconsin, pp. 37–56.

Nicholson R. V., Gillham R. W. and Reardon E. J. (1988) Pyrite oxidation in carbonate-buffered solution: 1. Experimental kinetics. *Geochim. Cosmochim. Acta* **52**, 1077–1085.

Nicholson R. V., Gillham R. W. and Reardon E. J. (1990) Pyrite oxidation in carbonate-buffered solutions: 2. Rate control by oxide coatings. *Geochim. Cosmochim. Acta* **54**, 395–402.

Pain D. J., Sanchez A. and Meharg A. A. (1998) The Donana ecological disaster: Contamination of a world heritage estuarine marsh ecosystem with acidified pyrite mine waste. *Sci. Total Environ.* **222**(1/2), 45.

Reedy B. J., Beattie J. K. and Lowson R. T. (1991) A vibrational spectroscopic 18O tracer study of pyrite oxidation. *Geochim. Cosmochim. Acta* **55**, 1609–1614.

Rosso K. M. (1998) The electronic structure and reactivity of sulfide surfaces: combining atomic-scale observations with theoretical calculations. *Doctoral Dissertation. Virginia Polytechnic Institute and State University*.

Schaufuss A. G., Nesbitt H. W., Kartio I., Laajalchto K., Bancroft G. M. and Szargan R. (1998a) Incipient oxidation of fractured pyrite surfaces in air. *J. Electron Spectosc. Related Phenomena* **96**, 69–82.

Scott T. B., Allen G. C., Heard P. J. and Randell M. G. (2003) Reduction of U(VI) to U(IV) on the surface of magnetite. *Geochim. Cosmochim. Acta* **69**(24), 5639–5646.

Scott T. B. (2005) The sorption of uranium onto iron bearing minerals. *Doctoral Dissertation, University of Bristol, United Kingdom*.

Simpson P. R. and Bowles J. F. W. (1977) Uranium mineralisation in the Witwatersrand and Dominion reef systems. In mineralogical aspects of ores. *Phil. Trans. R. Soc. Lond. A.* **286**, 527–548.

Singer P. C. and Stumm W. (1970) Acidic mine drainage. The rate-determining step. *Science* **167**, 1121.

Swanson V .E. (1956). Uranium in marine black shales of the United States. In: Contributions to the Geology of Uranium and Thorium by the United States Geological Survey and the Atomic Energy Commission for the United Nations International Conference on Peaceful Uses of Atomic Energy (eds. L. R. Page, H. E. Stocking and H. B. Smith). Geneva, Switzerland 1955. U.S. Geol. Surv. Prof. Pap., 300, pp. 451-456.

Taylor B. E. and Wheeler M. C. (1984) Stable isotope geochemistry of acid mine drainage: Experimental oxidation of pyrite. *Geochim. Cosmochim. Acta* **48**, 2669–2678.

Todd E. C., Sherman D. M. and Purton J. A. (2003) Surface oxidation of pyrite under ambient atmospheric and aqueous (pH 2 to 10) conditions: electronic structure and mineralogy from X-ray absorption spectroscopy. *Geochim. Cosmochim. Acta* **67**(5), 881–893.

Verbist J., Riga J., Tenret-Noël C., Pireaux J. J., d'Ursel G., Caudano R. and Derouane E. (1976). In *Plutonium and Other Actinides* (eds. H. Blank and R. Lindner), pp. 409–419. Plutonium and Other Actinides. North Holland, Amsterdam.

Wersin P., Hochella M. F., Persson P., Redden G., Leckie J. O. and Harris D. W. (1994) Interaction between aqueous uranium (VI) and sulfide minerals: spectroscopic evidence for sorption and reduction. *Geochim. Cosmochim. Acta* **58**, 2329.

Wagner C. D. (1988) Sensitivity factors for XPS analysis of surface atoms. *J. Electron. Spectosc. Related Phenomena* **328**, 99–102.

Associate editor: John Crusius